

Derivation and Validation of Digital Filter Performance for Front-End Electronics Design

Jae Chang Kim^a, Junehyung Lee Bernaski^a, Jae Young Jeong^a, Yong Kyun Kim^{a*}
^a Department of Nuclear Engineering, Hanyang University, Seoul, Korea
*Corresponding author: yk kim4@hanyang.ac.kr

***Keywords** : neutron detection, digital filter, recursive algorithm

1. Introduction

Differential Die-Away (DDA) method for quantification and management of spent fuel and Specific Nuclear Materials (SNM) has been developed in this study. The DDA method involves irradiating SNM with pulsed neutrons, measuring the resulting induced fission neutrons, and utilizing the difference in die-away time of the measured neutrons [1]. The aim is to minimize analog components and employ a ³He proportional counter with digital filters for neutron measurements. As a result, this paper presents the development and validation process of digital filters for neutron measurement.

2. Methods and Results

2.1 Characteristics of Neutron Detection using ³He Proportional Counter

The neutron measurement method using a ³He proportional counter is depicted in Fig. 1 [2]. The current signal generated within the detector is converted into a semi-step pulse with sufficient decay time using a charge-sensitive preamplifier. To counteract the pile-up effect where new pulses arrive before the previous one fully decays, a shaping amplifier is commonly employed to mold the signal. Subsequently, the peak identifications and the amplitude measurements using an MCA are accomplished to obtain the energy spectrum. Finally, the neutron classification is performed based on the values beyond the channel where the wall effect occurs.

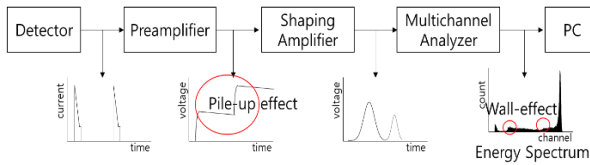


Fig. 1. Traditional neutron detection method using ³He proportional counter

The circuits commonly utilized in shaping amplifiers are CRⁿ-RC^m (n=1,2 m=1,2,3,4) circuits and CR_p¹-RC^m (m=1,2,3,4) circuits, as shown in Fig. 2. The CR¹-RC^m filter, referred to as a semi-Gaussian filter, generates a unipolar output signal and can be adjusted to achieve a faster baseline by shortening the decay time of the input signal. However, in the case of the CR¹-RC^m filter, undershooting can occur due to the long decay time of the input signal. To resolve this issue, the CR_p-RC^m

circuit, which involves parallelly connecting a resistor to the capacitor to perform pole-zero cancellation, can be employed [2]. The CR²-RC^m filters produce a bipolar output. This filters have a degraded noise performance compared with monopolar filters but in some situation is preferred because monopolar filters at high rates lead to a baseline shift, which can be reduced by a bipolar shape [3]. The role of the MCA involves applying a dynamic threshold method to the output signal of the digital filter, enabling the acquisition of an energy spectrum through appropriate computation time [4]. Thus, this paper derives twelve digital filters and validates their performance.

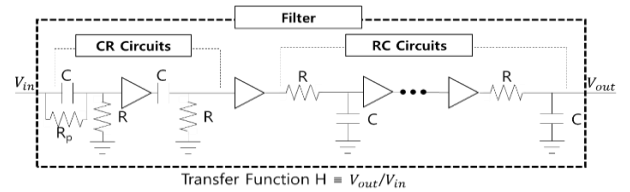


Fig. 2. Derivation of digital filter circuit and transfer function

2.2 Derivation of Digital Filters

The derivation of digital filter recursive algorithms requires a transfer function represented as the ratio between the output and input signals in Fig. 2. Kirchhoff's law is applied to the circuit of interest regions to obtain a transfer function in the continuous-time(t) domain. This t-domain transfer function is then transformed into the continuous-frequency(s) domain through Laplace transformation, and the results are represented in equations 1 and 2.

$$(1) H_{CR^n-RC^m}(s) = \frac{(RCs)^n}{(RCs+1)^{n+m}}$$

$$(2) H_{CR_p-RC^m}(s) = \frac{R(R_pCs+1)}{(R_p+R(R_pCs+1))(RCs+1)^m}$$

Subsequently, the continuous-frequency(s) domain transfer function is converted into the discrete domain(z) using the bilinear transformation among various methods. The time-shifting property of the z transformation is utilized to derive a recursive algorithm from the discrete domain transfer function [5].

2.3 Experiment Setting

An experiment shown in Fig. 3 was conducted to evaluate the performance of the digital filter. The setup included a ³He proportional counter with an effective

length of 30 cm and a radius of 1.5 cm and 4 atm operating pressure. Additionally, a 41.95 μCi ^{252}Cf source, a Canberra model 2006 preamplifier, and a 400 MHz FADC were utilized in the experiment. The output signal of the preamplifier was recorded using the FADC, and the recorded data underwent digital filter application. Furthermore, for verification of the counting rate, an identical experimental geometry was simulated using the MCNP6.1.

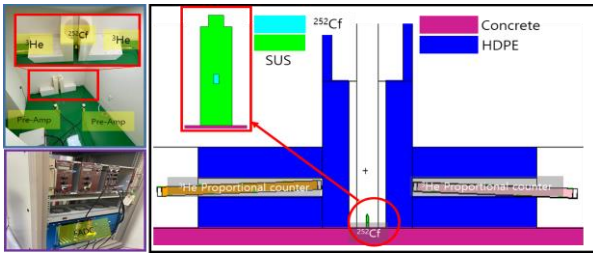


Fig. 3. Experiment and simulation geometry

2.4 Performance Evaluation of Recursive Algorithms

The response of the derived recursive algorithm to an ideal signal is depicted in Fig. 4. For the $\text{CR}^1\text{-RC}^m$ filter, the occurrence of undershooting is not observed in the case of a step pulse; however, undershooting is confirmed in the case of a tail pulse. On the other hand, employing the $\text{CR}_p\text{-RC}^m$ filter resulted in a proper return to the baseline.

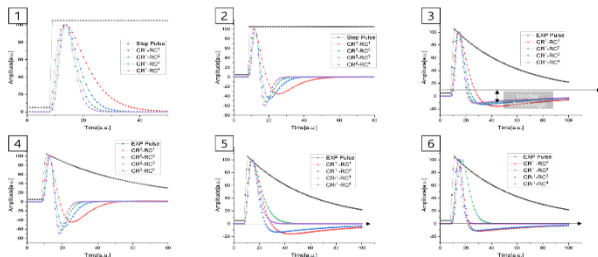


Fig. 4. Digital filter output for ideal signals

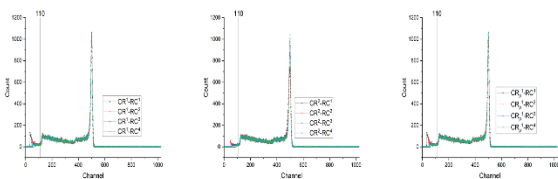


Fig. 5. Energy spectrum using digital filter

The energy spectrum obtained by applying the digital filter to the experiment is presented in Fig. 5. A dynamic threshold method was used to perform a peak search by adjusting the filter gain, and a full energy peak was ensured to exist in 500 out of 1024 channels. The count rate was calculated as the sum of values above channel 110, where the wall effect begins. Furthermore, the energy resolution was assessed at the full energy peak. Following these analyses, the computational time for

each filter and the simulation results are summarized in Table 1.

Table. 1. Evaluation results of the digital filter

Filter	Count rate [CPS]	Computing time [%]*	Resolution [%]
$\text{CR}^1\text{-RC}^1$	357.90	8.20	2.91
$\text{CR}^1\text{-RC}^2$	354.70	11.68	2.65
$\text{CR}^1\text{-RC}^3$	352.37	13.98	2.56
$\text{CR}^1\text{-RC}^4$	350.16	17.90	2.44
$\text{CR}^1\text{-RC}^1\text{-PoleZero}$	358.92	9.19	2.62
$\text{CR}^1\text{-RC}^2\text{-PoleZero}$	358.10	11.70	2.61
$\text{CR}^1\text{-RC}^3\text{-PoleZero}$	357.14	15.59	2.55
$\text{CR}^1\text{-RC}^4\text{-PoleZero}$	355.95	17.92	2.42
$\text{CR}^2\text{-RC}^1$	357.12	11.63	3.89
$\text{CR}^2\text{-RC}^2$	355.60	12.05	3.15
$\text{CR}^2\text{-RC}^3$	354.02	18.04	2.85
$\text{CR}^2\text{-RC}^4$	352.43	20.33	2.75
Simulation	353.53	* Filter Computing Time/Live Time \times 100	

3. Conclusions and Future Works

The outputs of the derived recursive algorithm are consistently deemed appropriate, and the neutron counting rate exhibited an error within 2% compared to the computational simulation while maintaining satisfactory resolution. Consequently, when designing the front-end electronics in the future, we intend to select an appropriate filter, considering the performance of the FPGA.

ACKNOWLEDGMENTS

This work was supported by the Nuclear Safety Research Program through the Korea Foundation Of Nuclear Safety(KoFONS) using the financial resource granted by the Nuclear Safety and Security Commission(NSSC) of the Republic of Korea. (No. 2106075)

REFERENCES

- [1] S. M. Thomas, et al. Development of Techniques for Spent Fuel Assay–Differential Dieaway Final Report. No. LA-UR-16-25686. Los Alamos National Lab.(LANL), Los Alamos, NM (United States), 2016.
- [2] G. F. Knoll, Radiation Detection and Measurement, John Wiley & Sons, New York, pp.595-598;630-642, 2010.
- [3] N. Mohammad. Signal processing for radiation detectors. John Wiley & Sons, pp.217-218, 2017.
- [4] Kamleitner, J., et al. "Comparative analysis of digital pulse processing methods at high count rates." Nuclear Instruments and Methods in Physics Research Section A: Accelerators, Spectrometers, Detectors and Associated Equipment 736 (2014): 88-98.
- [5] W. Alexander, et al. Digital Signal Processing: Principles, Algorithms and System Design, Academic Press, pp.73-75, 2016